A Predictive Control Framework for UAS Trajectory Planning Considering 4G/5G Communication Link Quality

Rui Zuo*, Zixi Wang*, Carlos E. Caicedo Bastidas[†], M. Cenk Gursoy*, Adrian Solomon[‡], Qinru Qiu*

*College of Engineering & Computer Science, Syracuse University

[†]School of Information Studies, Syracuse University

[‡]Thales Digital Aviation Customer Success and Innovation, Thales USA

Abstract—A reliable command and control (C2) data link is required for unmanned aircraft systems (UAS) operations in order to monitor the status and support the control of UAS. A practical realization of the C2 communication and mission data links for commercial UAS operations is via LTE/5G networks. While the trajectory of each UAS directly determines the flight distance and mission cost in terms of energy dissipation, it also has a strong correlation to the quality of the communication link provided by a serving base station, where quality is defined as the achieved signal-to-interference-plus-noise ratio (SINR) required to maintain the control link of the UAS. Due to signal interference and the use of RF spectrum resources, the trajectory of a UAS not only determines the communication link quality it will encounter, but also influences the link quality of other UAS in its vicinity. Therefore, effective UAS traffic management must plan the trajectory for a group of UAS taking into account the impact to the interference levels of other base stations and UAS communication links. In this paper, an SINR Aware Predictive Planning (SAPP) framework is presented for trajectory planning of UAS leveraging 4G/5G communication networks in a simulated environment. The goal is to minimize flight distance while ensuring a minimum required link quality for C2 communications between UAS and base stations. The predictive control approach is proposed to address the challenges of the time varying SINR caused by the interference from other UAS's communication. Experimental results show that the SAPP framework provides more than 3dB improvements on average for UAS communication parameters compared to traditional trajectory planning algorithms while still achieving shortest path trajectories and collision avoidance.

Index Terms—UAS, UAV Trajectory Planning, A*, Communication Quality

I. INTRODUCTION

General traffic planning for UAS (Unmanned Aircraft Systems) involves the search for an optimal path within certain constraints to avoid potential reduced separation events with manned aircraft, collisions with ground-based infrastructure, and to ensure mission safety. During most UAS operations, it is mission-critical to maintain a stable C2 link. The C2 link can be established over LTE/5G network services. To leverage these networks, several factors such as the location of LTE/5G ground base stations, the effective communication coverage areas and interference, among others, need to be considered. The high-bandwidth and low-latency communication capabilities offered by these networks are essential for

real-time control of UAVs, and in the context of LTE/5G, an important indicator for the quality of the communication link is the Signal-to-Interference-plus-Noise Ratio (SINR). High SINR values indicate a strong and reliable C2 link, while low SINR values can result in communication failure or delays, which can compromise the safety and effectiveness of UAV operations. Therefore, ensuring a high SINR is critical when planning trajectories using LTE/5G networks as the communication backbone. In this work, we propose an SINR Aware Predictive Planning (SAPP) framework to provide the best trajectory for each UAV with guaranteed SINR improvement while also preserving the benefits of collision avoidance and minimizing trajectory length, and we refer to such trajectory as Communication Optimized Trajectory (COT).

In order to compare candidate trajectories, or more accurately, candidate waypoints, prior knowledge of communication link quality of the environment is required to search for a COT before launching a new UAV, which makes the prediction model of SINR a necessity. With this motivation, we develop a prediction model that can accurately estimate the SINR of the downlink connections between a UAS and its attached base station based on their geographical location and the geographical locations of other base stations and UAS in the vicinity. The management of spectrum resources between base stations in our analysis is based on the Hard Frequency Reuse Method (HFRM) but it can be easily extended to other frequency reuse methods. For each downlink connection between the UAS and the attached base station, the model calculates the SINR as a composition of three variables, namely peak SINR (without interference), worst-case SINR due to interference, and the probability that another base station in the vicinity will transmit at the same time (i.e., the possibility of having interference). The model is able to predict the best-case link quality when there is no interference and also the worst-case SINR with the consideration of interference from neighboring base stations and UAS's. Neural network models are constructed and trained for the prediction of each variable. The predictions made by the models have a very high correlation (~ 0.98) with the simulated results. The model is flexible by design and can be applied to various combinations of communication link scenarios with different configurations.

Benefiting from our previous simulation platform [1], we can first analyze the most dominant factors that affect the communication quality from the simulation data. Then use the simulator to generate the training data to train the SINR prediction model.

Having an accurate SINR prediction model on hand enables us to work towards designing a trajectory planning algorithm to search for a COT. We further design a UAS traffic planning algorithm that utilizes the SINR predictor to evaluate the communication link quality during UAS trajectory planning. In addition to collision avoidance, the algorithm searches for the shortest path that can achieve a minimum acceptable level of communication link quality along the path. The predicted communication link quality is used by the A* (A-star) algorithm to search for the optimal path within spatio-temporal dimensions. A* [2] is a path search algorithm that in general does not take communication link parameters into consideration. In this paper, we propose a communication-enhanced version of A* (CommA*) that incorporates communication costs and constraints into the path search algorithm in order to improve performance in communication-constrained environments.

The rest of the paper is organized as the follows. Section II provides an overview of related work. In Section III, we inspect the five most dominant factors that affect the communication link quality in greater detail, followed by an introduction to SINR prediction models and a numerical evaluation of the models in Section IV. We discuss the background related to the A* algorithm and introduce the design details of the CommA* algorithm in Section V. In Section VI, we compare the experimental results of CommA* and A* algorithms under low, medium and high traffic load.

II. RELATED WORK

The increasing popularity of small unmanned aerial systems (sUAS) has brought to light several crucial and noteworthy concerns related to sUAS traffic management. As a result, various approaches and frameworks have been suggested to address these concerns.

The authors in [3] proposed a method based on optical flow to improve obstacle avoidance for sUAS. While there are more recent works using machine learning methods, a deep reinforcement learning framework that has the capability to perform energy-efficient way-point planning has been adopted in [4]. However, these works mainly targeted trajectory planning for a single UAV.

Trajectory planning for multiple UAVs has also been addressed in the literature. [5] and [6] used mixed integer linear programming to enable UAVs to find a feasible path that is collision free with shortest trajectory distance. UAV communications are not considered during the planning. [7] proposed a trajectory planning framework that is capable of meeting the constraints of no fly zones, static and dynamic obstacles and minimum communication link quality. However, a rather preliminary model is used to estimate the communication link quality.

The communication quality in cellular UAV communications is commonly measured by the signal-to-noise ratio (SNR) of the link between the unmanned aerial system (UAS) and the ground control station (GCS), as per recent studies. In [8], the authors propose an algorithm for optimizing the trajectory of a single UAS with the objective of achieving maximum energy efficiency while ensuring that the SNR of the connection between the UAS and base station remains above a predetermined threshold. On the other hand, [9] utilizes simulations to assess the communication quality based on a specific propagation model, which considers only the SNR parameter. However, SNR is not sufficient in measuring the quality of the wireless channel. A more accurate metric is the signal-to-interference-plus-noise ratio (SINR).

In this paper, we propose a trajectory planning that aims for a COT, where we include the experienced SINR along the trajectory as part of the quality metrics for the trajectory.

III. VARIABLES AFFECTING SINR

In the rest of the paper, we use downlink SINR as the metric for communication link quality. This is the SINR measured on the signal transmitted from the base station to the UAV. The downlink SINR, which we abbreviate as SINR in the remainder of the paper, is determined by S, the received downlink signal power spectral density (PSD); N, the noise PSD and I the PSD of the downlink interfering signals, as shown below:

$$SINR = \frac{S_{\rm Rx}}{N+I}.$$
 (1)

The notations for the above mentioned terms are as shown in Table I. In the following subsections, the dominating factors that impact the above mentioned terms are discussed.

A. Signal PSD

The signal PSD S_{Rx} is dominated by two major factors: the PSD from the transmitter S_{Tx} and the pathloss of the channel PL:

$$S_{\rm Rx} = \frac{S_{\rm Tx}}{PL}.$$
 (2)

 S_{Tx} , the PSD from the transmitter is determined by the total transmission power and allocation of the power across the used spectrum. We follow the common method where the transmission power is allocated uniformly across the entire active bandwidth, and the active bandwidth is determined by a frequency reuse method. Hence, the transmission power of the base station and the frequency reuse method jointly determine the transmission PSD. For the remainder of this paper, the Hard Frequency Reuse Method (HFRM) is considered. HFRM is a frequency reuse method that divides the entire frequency bandwidth into a few (usually 3) sub-bands, and assigns cells different orthogonal sub-bands such that the neighboring cells are completely separated in the frequency domain, as illustrated in Figure 1. The smallest level of granularity used for frequency assignment is a resource block (RB), and each RB spans 180kHz. In the later sections of this paper, the subband bandwidth is measured by RBs.

TABLE I VARIABLES IN SINR FORMULA

Variable notation	
S_{Rx}	The received downlink signal power spectral density(PSD).
I	The PSD of the downlink interfering signals
N	The noise PSD

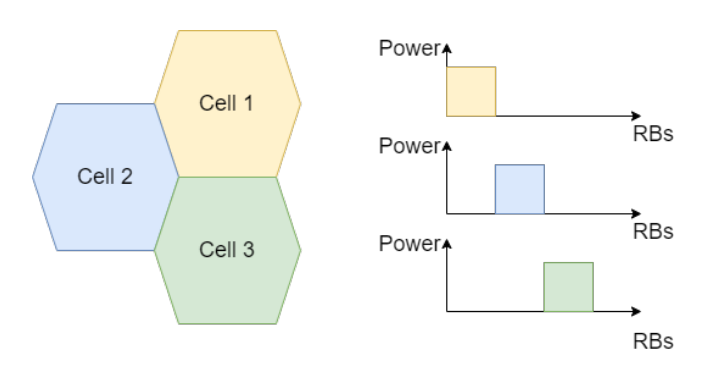


Fig. 1. HFRM assigns neighboring cells with orthogonal sub-bands such that they each enjoy a completely separated sub-band. Within the sub-band, power is distributed evenly across the sub-band bandwidth.

PL, the pathloss, describes the attenuation effects of the channel. According to the guidelines from 3GPP on enhanced LTE support for aerial vehicles [10], for UAVs flying at a height between 40 meters and 300 meters, the line of sight (LOS) probability is 1. Thus, the LOS path loss model for macro base stations in rural and urban scenarios, given as,

$$PL_{\text{RMa-AV-LOS}} = \max(23.9 - 1.8 \log_{10}(h_{\text{UT}}), 20)$$

$$\times \log_{10}(d_{3\text{D}}) + 20 \log_{10}(\frac{40\pi f_c}{3})$$
(3)

$$PL_{\text{UMa-AV-LOS}} = 28.0 + 22 \log_{10}(d_{3D}) + 20 \log_{10} f_c,$$
 (4)

are suitable for the scenarios that we will consider. In the above formulations, $h_{\rm UT}$ is the height of the UAV, d_{3D} is the 3D distance from the UAV to the corresponding base station and f_c is the carrier frequency.

It is evident that for both models, the distance between the UAV and the serving base station is the key factor.

B. Noise PSD

The noise power N is modeled by a fixed noise figure that describes the noise introduced by both the transmission device and the receiving device. We would like to mention that despite adopting the common method of modeling the channel noise with a fixed noise figure, such information remains unknown to the predictor. The impact of the noise is learned by the prediction models in Section IV via machine learning methods, without information about the underlying noise figure configuration.

C. PSD of Interfering Signals

The PSD of the downlink interfering signal, I, is dominated by the inter-cell interference generated by the signal from

other base stations serving other UAVs. The power of such interfering signals is affected by their respective transmission power and the pathloss experienced from the interfering base stations to the victim UAV, thus the transmission power of the interfering base stations and the distance between the victim UAV and the interfering base stations are two of the dominating factors. The inter-cell interference is also heavily affected by the frequency reuse method, i.e., how orthogonal sub-bands are assigned to adjacent cells such that intercell interference is mitigated. For instance, in HFRM, the configured sub-band bandwidth determines to which degree the sub-bands for adjacent cells are overlapping.

Moreover, interference is present only when the interfering base station is transmitting. The traffic pattern of the interfering base stations, i.e., whether the transmission occurs randomly or follows some periodic behavior, is critical to predicting the experienced SINR. In this work, we consider a scheduled traffic pattern where all the transmissions happen synchronously to simulate a worst case scenario, and a random traffic pattern of Poisson arrivals, where the transmission interval of each UAV associated with the interfering base stations follows an exponential distribution to simulate an average case.

IV. PREDICTION MODELS

As introduced in Section III, interference is a dominating factor in SINR prediction. However, unlike the other deterministic factors, the presence of interference is dependent on the transmission pattern of the other UAVs, which, in the real world, is random.

To develop the prediction models that enable SAPP, a fourstep process is adopted:

- First, a prediction model is trained for the peak SINR, which is the SINR achieved when there is no interference.
- Secondly, the factors affecting the worst-case SINR, which is the SINR achieved when there is constant interference from other base stations, is analyzed and the prediction model for the worst-case SINR is developed.
- Thirdly, the prediction model for interference probability, which predicts the probability of interference experience for a particular subject UAV, is developed and trained.
- Finally, the average SINR prediction model can be obtained by combining all above predictions.

All training data are acquired from simulations utilizing the integrated simulation platform developed in [1].

The platform is an air traffic and communication cosimulator, consisting of two components: i) a Multi-agent Air Traffic and Resource Usage Simulation (MATRUS) framework, based on the Repast agent-based simulation platform, that simulates UAS air traffic and collects UAS mobility information; and ii) a communications network simulator developed on top of the ns-3 platform and its LTE modules, that provides detailed and realistic cellular communication simulation under LTE protocols.

The co-simulation framework enables users to model various scenarios by adjusting parameters like base station locations, resource block count, and propagation models for urban or rural settings, along with mission profiles and nofly zone definitions. The integrated simulator can produce detailed communication link quality reports. These desirable features enables the training for our prediction models and the implementation of our proposed trajectory planning algorithm.

A. Peak SINR Prediction Model

Under the assumption that interference would always be absent, the peak SINR is mainly affected by the PSD from the Tx and the pathloss, as shown in (2). The two jointly determine the received signal PSD, i.e., the numerator of the SINR value as shown in (1). The pathloss is as shown in (3) and (4) for rural and urban scenarios, respectively. The value of the transmitted signal PSD and the pathloss can be further influenced by the variables stated in Table II.

A multi-layer perceptron model (MLP), with 1 input layer, 2 hidden layers and 1 output layer is trained for the peak SINR prediction. We define a vector of input $x_{\text{Serving eNB}}$ as

$$\mathbf{x}_{\text{Serving eNB}} = [d_{\text{serving}}, P, Bw, RB_{\text{used}}, RB_{\text{offset}}].$$
 (5)

We denote the peak SINR prediction model as $f_{Peak}(x_{Serving\ eNB})$.

The correlation between the true peak SINR value (i.e., the label of the data) acquired from simulations and the peak SINR value predicted by the model is shown in Figure 2. We achieve a correlation coefficient larger than 0.99, indicating that the predicted value is highly positively related to the label. The mean squared error (MSE) loss is less than 0.18, showing that the error made by the prediction model is small.

B. Worst-case SINR Prediction Model

As introduced in Section III, the downlink interference signals are essentially signals from other base stations intended to serve other UAVs. We first conduct various experiments exploring the impact of the number of other UAVs associated with (i.e. being served by) interfering base stations. The experiment was simulated with one base station serving the subject UAV, and one interfering base station serving various numbers of UAVs. All UAVs are scheduled to transmit at the same time, to ensure that interference is always present. The results are shown in Table III. It can be seen that the number of UAVs attached to the interfering base station had negligible impact on the SINR.

The factors in Table IV will be used to predict the percentage of SINR drop when a UAV suffers from interference from a number of interfering base stations, which is measured by

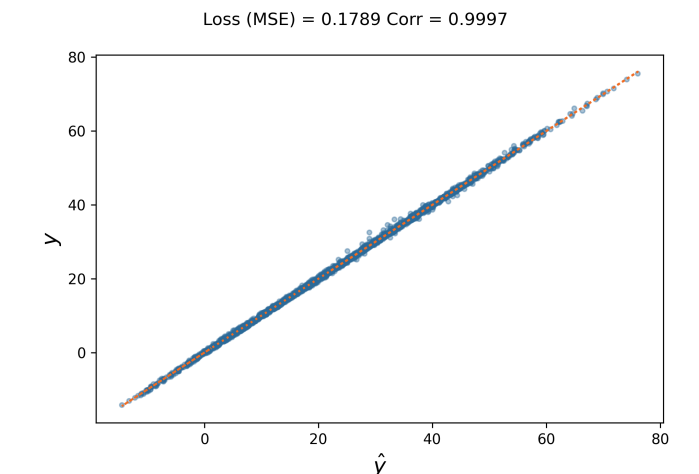


Fig. 2. Correlation figure for predicted peak SINR, where y represents true peak SINR value acquired from simulation (label); \hat{y} is the predicted peak SINR from the trained model.

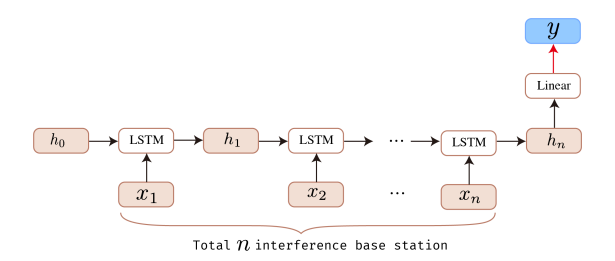


Fig. 3. The structure used for the prediction model for the worst-case SINR.

$$Drop = \frac{(SINR_{peak} - SINR_{worst})}{SINR_{peak}}.$$

In order to support an arbitrary number of interfering base stations, we build the predictor based on Long Short Term Memory (LSTM) model. Following the order from nearest to farthest, the features of the interfering base stations are fed into the LSTM model. The predicted drop percentage are calculated from the hidden state of LSTM using several layers of a fully connected network. The structure is illustrated in Figure 3. Theoretically, our model can support any number of interfering base stations with high accuracy.

We define a vector of input $x_{\text{Interfering base station}}$ as

$$x_{\text{Interfering eNB}} = \begin{bmatrix} x_1 \\ \vdots \\ x_n \end{bmatrix}$$
 (6)

$$\mathbf{x}_{i} = \begin{bmatrix} d_{i,Interferer} & P_{i} & Bw & RB_{used} & RB_{offset} \end{bmatrix}$$
 (7)

where n is number of interfering base stations.

We denote the drop percentage prediction model as $f_{Loss}(x_{\rm Interfering\ eNB})$. It is the ratio between the worst case SINR and the peak SINR of the UAV.

The correlation between the true drop percentage (the label of the data) acquired from simulations and the model predicted

TABLE II INPUT VARIABLES FOR PEAK SINR PREDICTION

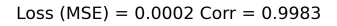
Base Station PSD	P	The transmission power of base station.	
	Bw	The bandwidth of base station.	
	RB_{used}	The number of RBs allocated for HFRM.	
	$RB_{ m offset}$	The RB offset in HFRM.	
Pathloss	$d_{Serving}$	The 3D distance between subject UAV and its serving base station, d_{3D} in section III.	

TABLE III
VARIOUS UAVS ATTACHED TO INTERFERING BASE STATION

Number of UAVs at interferer	SNR (no interference) (dB)	Worst-case SINR (dB)
1	33.46	32.64
3	33.36	32.64
5	33.46	32.64
7	33.46	32.63
9	33.46	32.63

TABLE IV
INPUT VARIABLES FOR WORST-CASE SINR PREDICTION

Interfering Base Station PSD	P	The transmission power of the interfering base station.
C	Bw	The bandwidth of interfering base station.
	$RB_{ m used}$	The number of RBs allocated for HFRM.
	$RB_{ m offset}$	The RB offset in HFRM.
Pathloss	$d_{ m Interferer}$	The distance between subject UAV and the interfering base station.



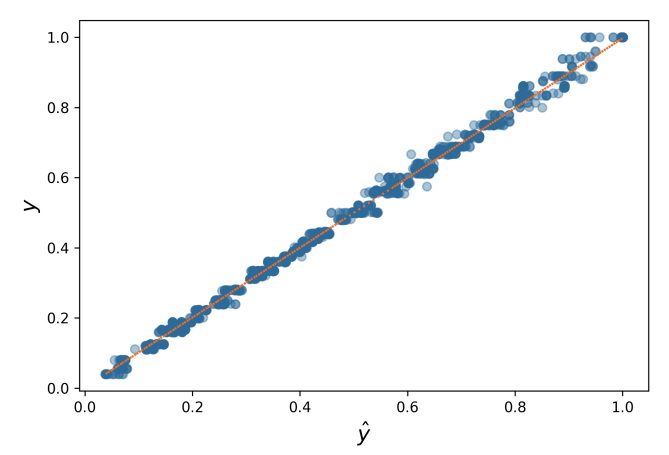


Fig. 4. Correlation figure for predicted worst-case SINR, where y represents true SINR drop percentage acquired from simulation (label); \hat{y} is the predicted SINR drop percentage from the trained model.

drop percentage is shown in Figure 4. We again achieve a correlation coefficient of larger than 0.99, which means that the predicted SINR drop percentage is highly positively related to the label. The mean squared error (MSE) loss is less than 0.0001, showing that the error of the prediction model is small.

By combining the predicted peak SINR and the predicted

percentage SINR drop, we can predict the worst-case SINR as

$$f_{\text{Worst-case}} = f_{Peak}(x_{\text{Serving eNB}}) \cdot f_{Loss}(x_{\text{Interfering eNB}}) \quad \ (8)$$

C. Interference Probability Model

In practical applications, the traffic pattern of UAVs would be highly random. As discussed in Section III, we adopt the assumption that all the UAVs' packet flows follow a Poisson pattern. That is, the interval between two transmissions for a UAV is an exponential random variable. Utilizing the simulation platform in [1], we implement this Poisson traffic pattern with an On/Off application in ns3. This application consists of two parameters: the OnTime for the duration of the transmission from the UAV and the OffTime for the interval between two transmissions. We always configure the OnTime as the exact time needed to transmit one packet, which is roughly 0.5ms, and the OffTime as the exponential random variable that gives the desired Poisson traffic pattern. Since data flow towards each UAV follows a Poisson traffic pattern, the number of UAVs attached to both the serving base station (sibling UAVs) and the interfering base station will impact the probability that the subject UAV will experience interference. The input variables for the probability prediction model are listed in Table V.

We acquire simulated probability by attaching random numbers of UAVs to the serving base station and the interfering base station. We then use the simulated probability as the label for the training data. The correlation between the measured probability of interference acquired from simulation (the label

Serving Base Station	n_{sib}	Number of Sibling UAVs	
	OnTime	The time to transmit one packet.	
	OffTime	The parameter of the exponential random variable determining the time interval between two transmissions.	
interfering Base Station	n_{intf}	Number of interfering UAVs	
	$On \r Time$	The time to transmit one packet.	
	OffTime	The parameter of the exponential random variable sampling the time interval between two transmissions.	

27

27

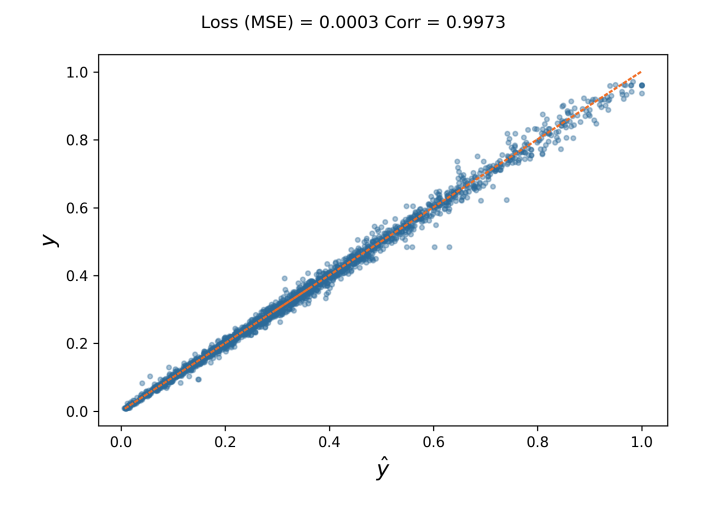


Fig. 5. Correlation figure for predicted interference probability, where y represents true simulated interference probability acquired from simulation (label); \hat{y} is the predicted interference probability from the trained model.

of the data) and the predicted interference probability is shown as figure 5. We achieved a higher correlation (greater than 0.997), and a low MSE error (low than 0.0002).

We denote the predicted interference probability as f_{Prob} . Combining it with predicted peak SINR and predicted percentage SINR drop, the average SINR can be calculated as

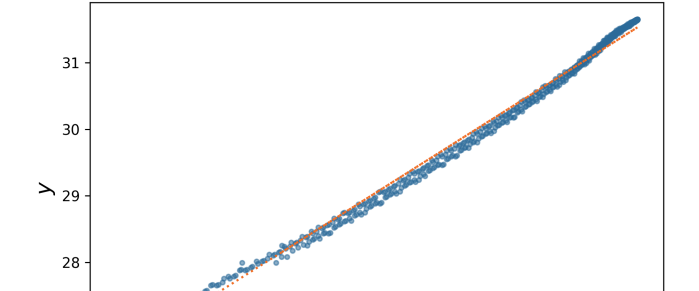
$$SINR_{avg} = f_{Peak} \cdot f_{Loss} \cdot f_{Prob} + f_{Peak} \cdot (1 - f_{Prob})$$
(9)

In addition to interference probability, average SINR is acquired from the simulation with the same settings above and the predicted average SINR is calculated following (9). The correlation between label and predicted average SINR is depicted in Figure 6 with correlation coefficient equal to 0.996 and MSE loss equal to 0.03.

V. A* WITH COMMUNICATION CONSIDERATION

A. Environment Assumptions

As mentioned in Section I, the goal of the CommA* routing algorithm is to provide a COT that guarantees improvement in terms of the SINR experienced along the trajectory, while maintaining collision avoidance and a comparable route length with respect to to A*.



Loss (MSE) = 0.1260 Corr = 0.9961

Fig. 6. Correlation figure for predicted average SINR, where y represents true simulated average SINR (label); \hat{y} is the predicted average SINR from the trained model

30

31

28

We adopt a proactive trajectory planning strategy that plans a conflict free trajectory for each sUAS at launch time or at the time when it enters the controlled airspace. As the trajectories for all UAVs in the designated airspace are planned by the corresponding control center, it can surely plan a COT for the incoming UAV if such a trajectory is feasible. If there is no possible path (i.e., there is collision on every possible path), the launch of such UAV will be delayed until a collision free path is available. As the SAPP is a proactive trajectory planner executed at the control center, power consumption or computing power would not be a limit. Any other possible air traffic constraint could be easily integrated as well.

We limit the trajectories to a Manhattan style to reduce the search space. Also, we adopt the "sky lane" concept proposed by [11]. Similarly, we divide the airspace into grids with uniform size. In the rest of the paper, we consider the scenario where the UAVs navigate through a 2D spatial plane. These limitations constrain the UAVs to fly at a constant speed and height, and to only make 90° turns. Note that the size of the grid cells naturally translates to the minimum separation of the UAVs for operational safety.

By considering time as one of the dimensions, the 2D spatial plane is then extended into a 3D spatio-temporal model, as depicted in Figure 7. Each cubic cell in the grid is located by

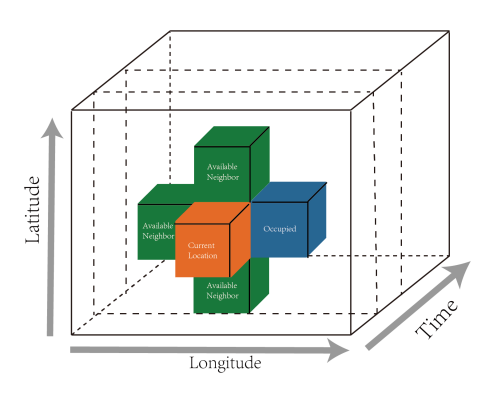


Fig. 7. Illustration of a temporal-spatial space. Note that each cell has 4 neighbors, all of which located on the next time step. For instance, the current cell (x,y,t) is marked blue. Cell $(x+w,y,t+\delta)$ is marked black because of its unavailability.

three coordinates: (latitude, longitude, time). Each cell would be of size (w, w, δ) , where w is the minimum separation between UAVs and δ is the time needed for a UAV to travel a distance of w. Note that δ is a constant as the UAVs are assumed to travel at a constant speed.

The environment consists of static obstacles (i.e., building, no-fly zones, etc.) and dynamic components with respect to occupation of a cell by another UAV and fluctuation of signal strength. For static obstacles, we use a 2D map for their storage, where each of the obstacles occupy a specific location. Since the static obstacles are time invariant, the information along the t axis is redundant and hence it can be eliminated. For the dynamic obstacles, we exploit their spatial sparsity and store them using hash tables along the t axis. Each location on the t axis is associated with a hash table, which stores the (x, y) coordinates of dynamic obstacles at the corresponding time.

B. Plain A* Routing Algorithm

The A* routing algorithm [2] is a heuristic routing algorithm that performs a best-first search. A* uses a combined evaluation function f(n) to estimate the cost of the best path that goes through node n:

$$f(n) = g(n) + h(n), \tag{10}$$

where n is a neighboring node of the current node, g(n) is the cost function from the source node to node n, h(n) is a heuristic estimation of the lowest cost from n to the destination. If the heuristic function h(n) satisfies the "admissible" property, which requires h(n) to never overestimate the cost to goal, then the A^* algorithm is guaranteed to find the least-costly route from the source node to the destination.

We utilize the A* routing algorithm to find the optimal path from the launching position to the destination in our spatiotemporal model. A UAV trajectory starts from a source grid cell (s_x, s_y, s_t) , and ends at any one of the destination grid cells (d_x, d_y) , where (s_x, s_y) and (d_x, d_y) are the coordinates of the launching position and destination grid cell, and t_s is the launch time.

The pseudo code for the original A* algorithm implemented on the discussed environment is shown in Algorithm 1. An instant refreshing mechanism is used such that the algorithm stores only the dynamic obstacles at or beyond the current time step. It is demonstrated in [2] that this saves from additional memory cost.

```
Algorithm 1: A* algorithm
```

```
Data: Starting Coordinates(s_x, s_y, s_t),
      Destination Coordinates(d_x, d_y)
Result: The optimal routing trajectory for one UAV
OpenList = \emptyset;
ClosedList = \emptyset;
ClosedList.add(start_position);
while OpenList \neq \emptyset do
   node = OpenList.poll();
   Instant Refreshing Mechanism;
   if node == destination then
       trajectory = retrieveTrajectory(node);
       break;
   end
   ClosedList.add(node);
   foreach neighbor \in CandidateSelection do
       if neighbor \in OpenList then
          neightbor = OpenList.get(neighbor)
       Calculate neightbor's NewMovementCost;
       if NewMovementCost <
        OldMovementCost || neighbor \notin OpenList
           update neighbor's MovementCost;
          update neighbor's DestinationCost;
          OverallCost =
            MovementCost + DestinationCost;
       end
       if neighbor \notin OpenList then
          OpenList.add(neighbot);
       end
   end
end
foreach position \in trajectory do
   mark OBSTACLE in 3D_dynamic_projection;
end
return trajectory;
```

C. Communication Enhanced A*

The accurate prediction models introduced in Section IV enables us to design a communication enhanced A* routing algorithm, which takes into consideration the communication link quality along the trajectory while maintaining the virtues of a short flight distance and collision avoidance.

Algorithm 2: Candidate Selection

To achieve such a goal, the evaluation functions of the A* algorithm is modified as follows:

$$g(n) = g(n-1) + \max(1 + \frac{s_{th} - s(n)}{s_{th}}, 0)$$
 (11)

$$h(n) = \max(1 + \frac{s_{th} - s(n, dst)}{s_{th}}, 0) \times d(n, dst)$$
 (12)

where s(n) is the communication link quality at location n, s(n,dst) is the average communication link quality in the area between location n and the destination, s_{th} is the threshold for communication link quality, and d(n,dst) is the Manhattan distance from n to the destination. Note that s_{th} is left open for a user defined, mission-dependent parameter.

Note further that we leave the definition of "communication link quality" open to any of the three SINR values introduced in Section IV. s(n) and s(n,dst) could be the estimated peak SINR (i.e., no interference at all), worst SINR (the case of always being interfered) or the average SINR (the expected SINR, where the expectation is taken over the randomness introduced by random transmission from other UAVs).

The rationale behind such modifications is to penalize the trajectory where the communication link quality is below s_{th} by increasing its distance cost and decreasing it if it is above the threshold.

VI. EXPERIMENTAL RESULTS

In the following experiments, an urban setting near Watford City, ND is considered. A map of this area is given in Figure 8. We have one launching area colored red on the west of the map and one landing area serving as the destination, colored purple on the east of the map. There are 4 base stations located in this area, and they are located at the red markers at the center of the green circles.

As discussed in Section V, all the UAVs in the following experiments fly at a fixed altitude of 100 meters and a fixed speed of 18m/s. The transmission powers of the base station and UAS are fixed at 40dBm and 15dBm, respectively. We use



Fig. 8. A map for the considered urban area near Watford City. The red launching area is located in the northeast of the map. The smaller purple destination is located in the east of the map. The four base stations are located at the red markers in the center of the green circles.

the 3GPP urban macro model in [10] as the propagation model. The total bandwidth supports 15 RBs, and the frequency management is done via HFRM with the subband bandwidth set as 6 RBs.

As discussed previously, we adopt a spatio-temporal model in the environment for trajectory planning. The grid length for the spatial grid is 90 meters, i.e., the 2D spatial plane is divided into grids of size 90×90 , and the length in the temporal dimension is the corresponding time for the UAV to travel from one grid to a neighboring grid.

We then conduct experiments involving different traffic patterns using different trajectory planning algorithms, where, for CommA*, we further vary the prediction models used for the SINR evaluation s(n), s(n, dst) in equations (11) and (12). We measure the SINR experienced along the trajectory by calculating the percentage of the trajectory where the SINR is above a threshold of 30dB. Note that there are UAVs launched from the launching area and routed to the destination, which we refer to as the subject UAVs. In addition to these UAVs, there are also other UAVs attached to these base stations, these UAVs are used to simulate UAVs performing other missions and their communications activity will generate interference.

A. No Interference

The results in Table VI are acquired using the aforementioned experimental setup, but with no interference present at all. We launch 1 UAV from the launching zone and observe the trajectory planning offered by the A* and CommA*, where the SINR evaluation s(n), s(n, dst) in equations (11) and (12) is acquired from the peak SINR predictor.

B. Persistent Interference

The results presented in Table VII are acquired with a traffic pattern where the interfering base stations have scheduled transmissions that are perfectly synchronous with the scheduled transmission from the serving base station to the subject UAV. We configure that each base station transmits to its 10 attached UAVs at time $t_o + n \cdot \Delta t$, and the subject UAV receives packets from its serving base station at time $t_o + n \cdot \Delta t$ as well.

TABLE VI ONE UAV, NO INTERFERENCE

		Average SINR along trajectory(dB)	Route Length(km)	SINR above threshold(%)
1	A*	31.694923	8.91	92.1844%
1	CommA*(peak SINR)	32.371898	9.63	93.9759%

This configuration leads to the persistent downlink interference experienced by the subject UAV.

We then launch 1 UAV from the launching zone and observe the trajectory planning offered by the A* and CommA*, where the SINR evaluation s(n), s(n, dst) in equations (11) and (12) is acquired from the worst-case SINR predictor.

C. Random Interference

We then configure a random traffic pattern, where the base stations transmit randomly to their attached UAVs. The interval between two packets sent for a particular UAV is set to be an exponential random variable with a mean of 100ms. Again, in addition to the launched subject UAVs, we attach each base station with 10 other UAVs to generate downlink interference. These UAVs adopt the same traffic pattern, i.e., the base station transmits to them in the same way they transmit to the subject UAVs. Note that since interference is only present when there are interfering base station transmitting, the subject UAVs would experience random interference within such setups.

We conduct experiments with light, medium and high traffic loads, corresponding to 15, 50 and 100 UAVs launched from the launching areas. We perform trajectory planning for each traffic load using original A*, CommA*(peak SINR), CommA*(worst-case SINR) and CommA*(average SINR), where the configurations in between parentheses denote which predictor is used for the SINR evaluation s(n), s(n, dst) in equations (11) and (12).

The results are provided in Table VIII. The numerical results reported in Table VIII are averaged over all subject UAVs. Interestingly, with medium or high travel traffic volume, routing algorithms based on the worst-case SINR prediction give the best results. This is because, like all A* algorithms, the CommA* is a greedy algorithm. When planning UAV trajectories, it only considers the interference caused by the UAVs that have already been launched. It ignores the potential interference that will be introduced by the UAVs that will enter the air space at a later time. As a result, the actual SINR the UAV experiences is always lower than that the algorithm estimated during the planning time. Hence a planning algorithm based on the worst-case SINR works better because it provisions for potential further SINR degradation. Such provisioning is not necessary when the traffic is light. That is why the CommA* performs the best with the average SINR prediction instead of the worst-case SINR prediction under light traffic.

VII. CONCLUSION

In this paper, we have proposed SAPP framework using a communication aware A* routing algorithm for UAS trajectory

planning using 4G/5G cellular networks. The proposed framework includes accurate prediction models trained from simulations involving detailed communication metrics, enabling the accurate prediction of the peak SINR, the worst-case SINR and the average SINR. With the mentioned prediction models, we developed a CommA* algorithm that takes the experienced communication link quality along the trajectory into consideration, and plans for a communication optimized trajectory. While maintaining the merit of collision avoidance and short flight distance, CommA* demonstrated a substantial improvement in communication link quality in the experiments conducted based on real word scenarios. Moreover, we note that while the prediction models were trained under HFRM, they can be easily extended to other spectrum management schemes.

ACKNOWLEDGEMENT

This work is partially supported by the National Science Foundation I/UCRC ASIC (Alternative Sustainable and Intelligent Computing) Center (CNS-1822165).

REFERENCES

- [1] R. Zuo, Z. Wang, C. Luo, C. Caicedo, M. C. Gursoy, Q. Qiu, and A. Solomon, "An integrated simulation platform for the analysis of uas bylos operations supported by 4g/5g communications," in 2022 Integrated Communication, Navigation and Surveillance Conference (ICNS), 2022, pp. 1–12.
- [2] P. E. Hart, N. J. Nilsson, and B. Raphael, "A formal basis for the heuristic determination of minimum cost paths," *IEEE Transactions on Systems Science and Cybernetics*, vol. 4, no. 2, pp. 100–107, 1968.
- [3] C. Wang, W. Liu, and M. Q.-H. Meng, "Obstacle avoidance for quadrotor using improved method based on optical flow," in 2015 IEEE International Conference on Information and Automation, 2015, pp. 1674–1679.
- [4] H. Eslamiat, Y. Li, N. Wang, A. K. Sanyal, and Q. Qiu, "Autonomous waypoint planning, optimal trajectory generation and nonlinear tracking control for multi-rotor uavs," in 2019 18th European Control Conference (ECC), 2019, pp. 2695–2700.
- [5] M. Radmanesh, M. Kumar, A. Nemati, and M. Sarim, "Dynamic optimal uav trajectory planning in the national airspace system via mixed integer linear programming," *Proceedings of the Institution of Mechanical Engineers, Part G: Journal of Aerospace Engineering*, vol. 230, no. 9, pp. 1668–1682, 2016.
- [6] B. D. Song, J. Kim, and J. R. Morrison, "Rolling horizon path planning of an autonomous system of uavs for persistent cooperative service: Milp formulation and efficient heuristics," *Journal of Intelligent & Robotic Systems*, vol. 84, pp. 241–258, 2016.
- [7] Z. Zhao, Z. Jin, C. Luo, H. Fang, F. Basti, M. C. Gursoy, C. Caicedo, and Q. Qiu, "Temporal and spatial routing for large scale safe and connected uas traffic management in urban areas," in 2019 IEEE 25th International Conference on Embedded and Real-Time Computing Systems and Applications (RTCSA), 2019, pp. 1–6.
- [8] S. Zhang, Y. Zeng, and R. Zhang, "Cellular-enabled uav communication: A connectivity-constrained trajectory optimization perspective," *IEEE Transactions on Communications*, vol. 67, no. 3, pp. 2580–2604, 2019.
- [9] Z. Zhao, C. Luo, J. Zhao, Q. Qiu, M. C. Gursoy, C. Caicedo, and F. Basti, "A simulation framework for fast design space exploration of unmanned air system traffic management policies," in 2019 Integrated Communications, Navigation and Surveillance Conference (ICNS), 2019, pp. 1–10.

TABLE VII ONE UAV, PERSISTENT INTERFERENCE

		Average SINR along trajectory(dB)	Route Length(km)	SINR above threshold(%)
1	A*	29.247628	8.91	35.3414%
1	CommA*(worst-case SINR)	29.764992	9.09	54.509%

TABLE VIII RANDOM INTERFERENCE

Traffic Load		Average SINR along trajectory(dB)	Route Length(km)	SINR above threshold(%)
	A*	30.061219	9.585	51.3452%
Liab+(15)	CommA*(peak SINR)	30.079100	12.024	51.5940%
Light(15)	CommA*(worst-case SINR)	30.253960	11.9313	51.9914%
	CommA*(avg SINR)	30.485796	11.9637	56.3248%
	A*	29.722920	9.6912	47.2707%
Madium(50)	CommA*(peak SINR)	30.065327	11.9916	49.1959%
Medium(50)	CommA*(worst-case SINR)	30.187087	11.9232	53.2901%
	CommA*(avg SINR)	30.109362	11.7936	51.2455%
	A*	29.681577	9.7155	45.3052%
High(100)	CommA*(peak SINR)	30.133726	11.7144	51.1256%
	CommA*(worst-case SINR)	30.171082	11.5533	51.9046%
	CommA*(avg SINR)	30.135238	11.7909	50.8292%

TABLE IX NEW THRESHOLD

Traffic Load		Average SINR along trajectory(dB)	Route Length(km)	SINR above threshold(%)
	A*	29.763123	9.576	95.4242%
Light(15,	CommA*(peak SINR)	30.404998	12.5874	99.9317%
25.711)	CommA*(worst-case SINR)	30.505595	12.78	99.9053%
	CommA*(avg SINR)	30.406063	12.7557	100%
	A*	29.882095	9.5796	99.6098%
Medium(50,	CommA*(peak SINR)	30.363959	12.6612	99.9670%
24.979)	CommA*(worst-case SINR)	30.390324	12.4596	99.9666%
	CommA*(avg SINR)	30.267168	12.6	100%
	A*	29.930781	9.5382	96.1734%
Medium(100,	CommA*(peak SINR)	30.723548	12.9168	99.9858%
24.945)	CommA*(worst-case SINR)	30.36669	12.096	99.9670%
	CommA*(avg SINR)	30.372064	12.429	100%

 ^{[10] 3}GPP 36.777 "Enhanced LTE Support for Aerial Vehicles".
 [11] D.-S. Jang, C. A. Ippolito, S. Sankararaman, and V. Stepanyan,
 Concepts of Airspace Structures and System Analysis for UAS Traffic flows for Urban Areas. [Online]. Available: https://arc.aiaa.org/doi/abs/10.2514/6.2017-0449